EPJ Web of Conferences **365**, 05001 (2026) https://doi.org/10.1051/epjconf/202636505001
BPU12 Congress

Drell-Yan Production Using a New Approach PDF2ISR in the PYTHIA Event Generator

Dušan Subotić[1,*], *Hannes* Jung[2,3,**], and *Nataša* Raičević[1,***]

[1]Faculty of Science and Mathematics, University of Montenegro, Podgorica, Montenegro
[2]University of Antwerp, Antwerp, Belgium
[3]II. Institut für Theoretische Physik, Universität Hamburg, Hamburg, Germany

Abstract. We present PDF2ISR, a new method for constructing an initial parton shower consistent with parton densities, applied to Drell–Yan production. Implemented in the PYTHIA8 event generator, it incorporates the Parton Branching framework to modify the initial-state shower. Predictions are systematically validated against those from the CASCADE3 generator, which also employs the Parton Branching method and the same parton densities, including transverse-momentum–dependent distributions. After confirming the consistency of the modified initial-state showers with the Parton Branching method, we apply PDF2ISR to generate full Drell–Yan events with radiation included at each step and compare the resulting cross sections as a function of the pair's transverse momentum with the latest LHC measurements.

1 Introduction

The Drell-Yan (DY) pair production process, involving the creation of a lepton pair through a quark-antiquark annihilation in hadronic collisions, provides an excellent environment for studying various Quantum Chromodynamics (QCD) effects. In particular, the transverse momentum (p_T) distribution of DY pairs, especially at low p_T values, is highly sensitive to non-perturbative contributions, such as the treatment of inital state radiation (ISR) and the intrinsic transverse momentum of partons (intrinsic-k_T).

Standard Monte Carlo (MC) event generators, such as PYTHIA8 [1, 2] and HERWIG [3, 4], simulate ISR through parton showers that evolve backward from the hard scattering to the incoming hadrons, using collinear parton distribution functions (PDFs) as input. While highly successful, these approaches face challenges in consistently describing both collinear and transverse momentum dynamics, primarily in the non-perturbative region dominated by soft gluon emissions. In many ISR models, the intrinsic-k_T width is given an arbitrary energy dependence, potentially hiding the underlying QCD behavior.

Modern approaches, such as the Parton Branching (PB) method [5, 6], incorporate transverse-momentum–dependent (TMD) PDFs, allowing a more consistent treatment of non-perturbative transverse-momentum effects in ISR. The PB method provides a framework to determine TMDs by iteratively solving the DGLAP [7] evolution equations. Recently, the

*e-mail: dusan.sub@ucg.ac.me
**e-mail: hannes.jung@desy.de
***e-mail: natasar@ucg.ac.me

PDF2ISR [8] approach has been proposed to implement an ISR model in PYTHIA8 whose backward evolution is fully consistent with the forward evolution of the collinear PDFs in the PB method. This framework ensures that the ISR-generated TMDs match those obtained directly from the PB evolution, provided that the same evolution parameters and splitting functions are used. Initial studies have shown excellent agreement between PB and PDF2ISR predictions, both at leading order (LO) and next-to-leading order (NLO) accuracy.

In this paper, we present the first application of the PDF2ISR approach to the real Drell-Yan production process in proton-proton collisions. Using recent measurements from the LHC [9] as a benchmark, we compare the transverse momentum distributions obtained from PDF2ISR with those from the PB method and with experimental data. This provides a test of the consistency between the two approaches and of their ability to accurately describe the ISR-sensitive region of the DY pair p_T spectrum.

2 PB Method and TMDs

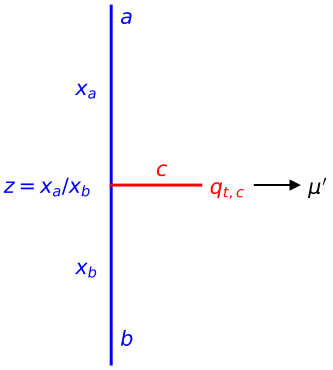

Figure 1. A single branching step in the PB method modelling.

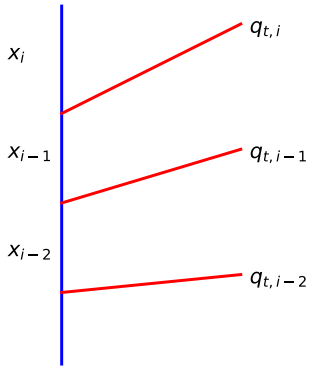

Figure 2. More branching steps, with angular ordering respected.

The PB method models the evolution of partons inside a hadron as a series of single branching steps (Fig. 1), where parton b, carrying momentum fraction x_b of the hadron, undergoes a splitting into two daughter partons: a, which continues the splitting chain and carries momentum fraction x_a, and c, which is emitted and carries transverse momentum $q_{t,c}$, which sets the branching scale μ'. Multiple such branchings build up the parton shower (Fig. 2). A key feature of the PB method is angular ordering, meaning emission angles increase with each step. This ensures the effects of soft gluon coherence are correctly reflected. Resolvable and non-resolvable emissions are defined by the parameter z_M, which is the maximum transferred momentum fraction, z, allowed in a single resolvable branching. With angular ordering used, the evolution scale is related to the transverse momentum of the emitted parton by:

$$\mu = \frac{q_t}{1-z}\,. \tag{1}$$

Parton evolution is expressed in terms or resolvable, real emission DGLAP splitting functions, P_{ab}, and Sudakov form factors, Δ_a, which give the probability to evolve from one scale

to another without resolvable emissions:

$$\Delta_a(z_M, \mu^2, \mu_0^2) = \exp\Big(- \sum_b \int_{\mu_0^2}^{\mu^2} \frac{d\mu'^2}{\mu'^2} \int_0^{z_M} dz\, z\, P_{ba}^{(R)}(\alpha_s, z)\Big). \tag{2}$$

The TMD, for a parton a, with the longitudinal momentum fraction x of the hadron, and the transverse momentum $\mathbf{k}$, evaluated at the scale μ, is given by:

$$\begin{aligned}\mathcal{A}_a(x, \mathbf{k}, \mu^2) &= \Delta_a(\mu^2)\, \mathcal{A}_a(x, \mathbf{k}, \mu_0^2) \\ &+ \sum_b \int_{\mu_0}^{\mu} \frac{d^2\mu'}{\pi\mu'^2} \frac{\Delta_a(\mu^2)}{\Delta_a(\mu'^2)} \times \int_x^{z_M} \frac{dz}{z} P_{ab}^{(R)}(\alpha_s, z)\, \mathcal{A}_b\Big(\frac{x}{z}, \mathbf{k} + (1-z)\boldsymbol{\mu'}, \mu'^2\Big),\end{aligned} \tag{3}$$

where $\mathcal{A}_a(x, \mathbf{k}, \mu_0^2)$ is the TMD at the starting scale μ_0, which is a non-perturbative boundary condition to the evolution equation, determined from experimental data. By integrating $\mathcal{A}_a(x, \mathbf{k}, \mu^2)$ over all $\mathbf{k}$, collinear PDFs, $f_a(x, \mu^2)$, are obtained.

In Eqs. 2 and 3, the scale for the strong coupling α_s is a function of the branching variables. Two cases are considered in the PB method:

$$\text{i)} \quad \alpha_s = \alpha_s(\mu'^2)\,, \tag{4}$$

$$\text{ii)} \quad \alpha_s = \alpha_s(\mu'^2(1-z)^2) = \alpha_s(q_t^2)\,. \tag{5}$$

For these two cases, different TMDs are generated: PB-NLO-2018 Set1 and PB-NLO-2018 Set2. It was found that PB-NLO-2018 Set2 provides a more accurate description of the experimental data[13].

In parton evolution, intrinsic-k_T is modelled by a Gaussian distribution with a width σ, which is related to the q_s parameter used in the PB method by:

$$\sigma^2 = \frac{q_s^2}{2}\,. \tag{6}$$

Then, given the collinear PDF $f_a(x, \mu_0^2)$ at the starting scale, the TMD has the form:

$$\mathcal{A}_a(x, \mathbf{k}, \mu_0^2) = f_a(x, \mu_0^2) \cdot \frac{\exp\Big(- \frac{|\mathbf{k}^2|}{q_s^2}\Big)}{(\pi q_s^2)^{\frac{1}{2}}}\,. \tag{7}$$

For standard shower-based event generators, the parameter q_s was extracted for different center-of-mass energies $\sqrt{s}$, and an increase of intrinsic-k_T width with energy was observed, independently of the tune that was used as shown in the recent publication [10]. In contrast to that, the results from CASCADE3 [11], which is based on the PB method, show only a very mild dependence [12]. A possible reason for this disagreement could be the exclusion of soft gluon emissions in standard generators, with the goal of avoiding potential divergences. The minimal transverse momentum of a parton in a single branching in the PB method is determined by the parameter q_0. Larger q_0 values mean that more soft gluon emissions are excluded. By varying this parameter, it is possible to mimic standard generators within the PB method, which led to the conclusions that the intrinsic-k_T width parameter increases with $\sqrt{s}$ for $q_0 > 0$, and the slope of the dependence increases as q_0 increases [13]. More extensive studies were conducted to investigate the impact of the Sudakov form factor on this behavior, including its scale dependence [14, 15]. The extracted values of the intrinsic-kT width are not purely intrinsic; rather, they result from the interplay of two non-perturbative processes: the internal transverse motion of partons and multiple soft gluon emissions.

3 PDF2ISR Approach

The PDF2ISR approach [8] is designed to modify the PYTHIA8 parton shower, so that its backward evolution is fully consistent with the PB forward evolution. The key idea is that TMDs from PB are, by construction, consistent with collinear PDFs, when integrated over **k**. In order to use this approach, initial state radiation in PYTHIA8 needs to be reconfigured to match the PB method. We need to use the same α_s treatment and apply angular ordering instead of previously used transverse momentum ordering.

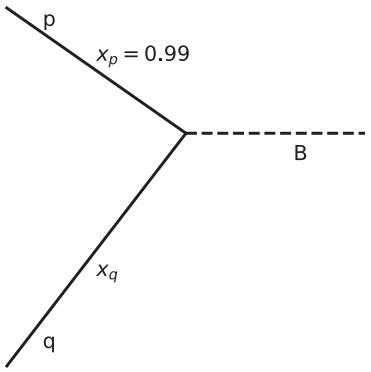

Figure 3. A diagram of the "toy model" process $p + q \to B$.

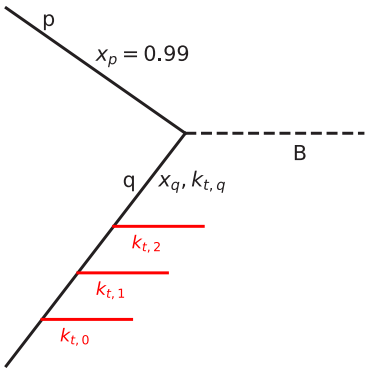

Figure 4. Process $p + q \to B$, with a parton shower from one side.

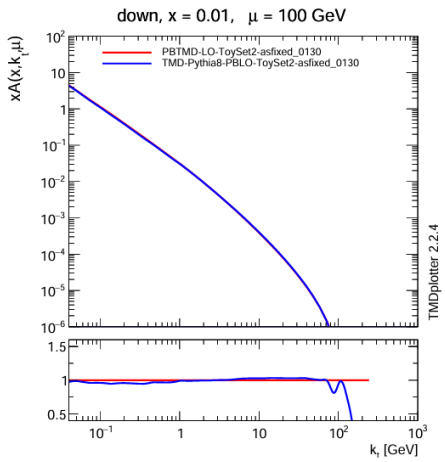

Figure 5. TMDs for down quarks with fixed $x = 0.01$ and $\mu = 100$ GeV at LO accuracy [8], with kind permission of The European Physics Journal (EPJ).

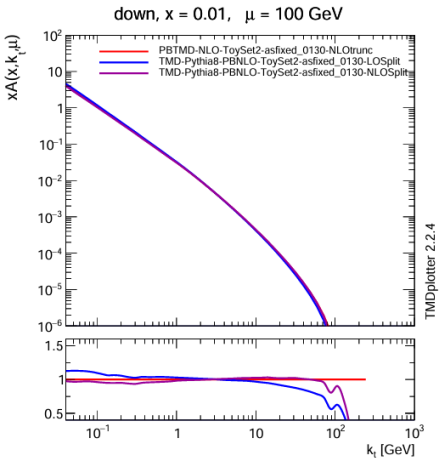

Figure 6. TMDs for down quarks with fixed $x = 0.01$ and $\mu = 100$ GeV at NLO accuracy [8], with kind permission of The European Physics Journal (EPJ).

The first validation test of the PDF2ISR approach was performed in Ref. [8] using a simplified "toy model". It is described by a process $p + q \to B$ (Fig. 3), where one of the

initial partons has a fixed momentum fraction $x_p = 0.99$, and the other has different x_q values. The produced boson B is unphysical, as it couples both to quarks and gluons. The scale μ associated with the process is generated across a wide range. Only the incoming parton q develops an initial-state shower and contributes to the boson's transverse momentum (Fig. 4). In this case, the boson's transverse momentum coincides with that of parton q, from which the relevant TMD is determined.

A very good agreement was observed between TMDs from the PB method and the PDF2ISR approach at LO accuracy (Fig 5). When they were compared at NLO accuracy, it was shown that NLO splitting functions must also be used for consistency (Fig 6).

4 Validation of PDF2ISR in DY production

As the first step in the validation study, we compared the PB method and the PDF2ISR approach, using DY pair production at LHC. We used the same phase space as in the most recent CMS measurements [9] of the Drell–Yan cross section as a function of the pair transverse momentum in proton–proton collisions at $\sqrt{s} = 13$ TeV covering five invariant mass ranges: $50 < m_{\ell\ell} < 76$ GeV, $76 < m_{\ell\ell} < 106$ GeV, $106 < m_{\ell\ell} < 170$ GeV, $170 < m_{\ell\ell} < 350$ GeV, and $350 < m_{\ell\ell} < 1000$ GeV. For this comparisson, we turned off multi-parton interaction (MPI) and final state radiation (FSR), so we isolate the effect of ISR on the DY pair $p_T(\ell\ell)$ spectra. A comparison of the differential cross sections as functions of $p_T(\ell\ell)$ in the five invariant mass bins is shown in Fig. 7. The figure confirms the consistency between the two approaches and demonstrates the correct implementation of the procedure in PDF2ISR.

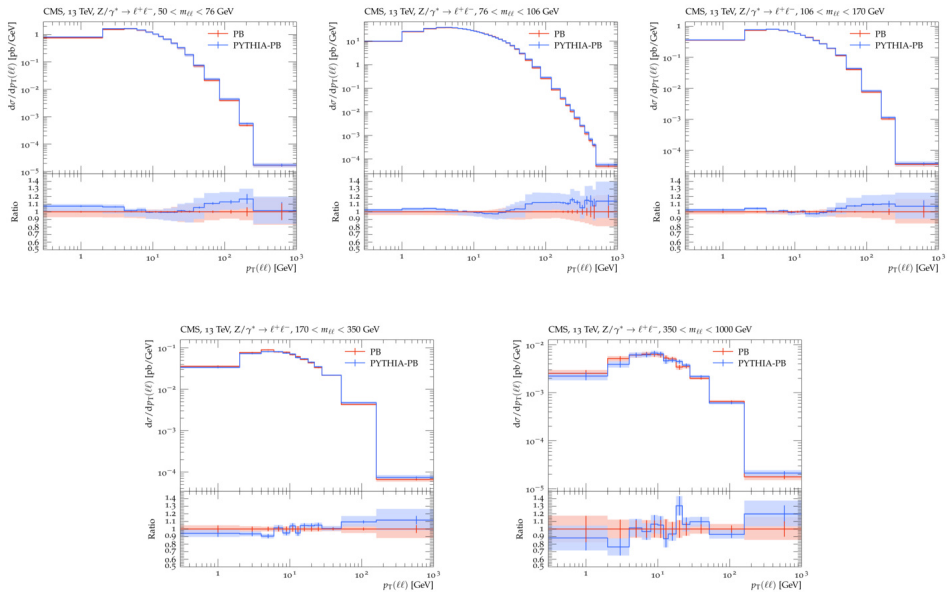

Figure 7. Comparison of the Drell–Yan cross sections as functions of the pair transverse momentum in proton–proton collisions at $\sqrt{s} = 13$ TeV across five invariant mass bins, between predictions from the Parton Branching method in CASCADE3 and the PDF2ISR approach implemented in PYTHIA8. The invariant mass and transverse-momentum bins of the pairs are chosen as in Ref. [9].

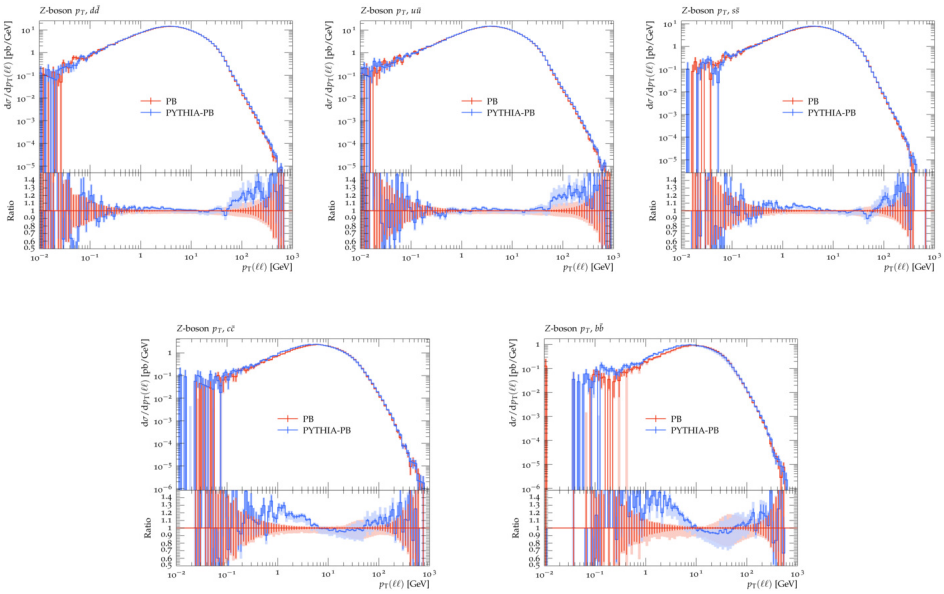

Figure 8. Comparison of the Drell–Yan cross sections from individual quark-flavour contributions as functions of the pair transverse momentum in proton–proton collisions at $\sqrt{s} = 13$ TeV in the Z-peak region, between predictions from the Parton Branching method in CASCADE3 and the PDF2ISR approach implemented in PYTHIA8.

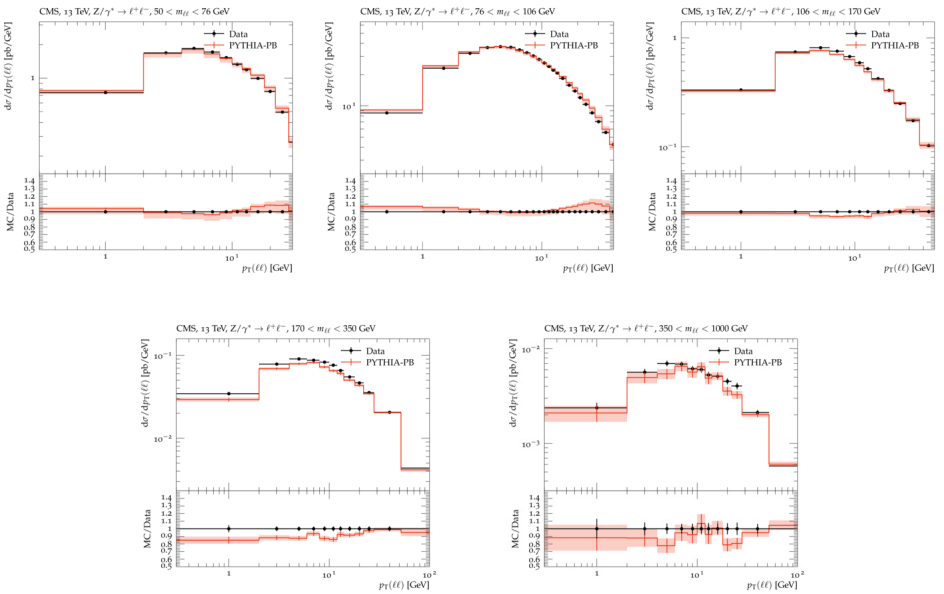

Figure 9. Comparison of the measured Drell–Yan cross sections as functions of the pair transverse momentum in proton–proton collisions at $\sqrt{s} = 13$ TeV, across five invariant mass bins [9], with predictions from the PDF2ISR approach.

To study the impact of the new ISR approach on individual quark flavours, we decomposed the Drell–Yan pair production into contributions from each quark flavour. Fig. 8 shows the contribution of an initial state quark and antiquark with a specific flavour forming the DY pair. For heavy flavours, charm and bottom, the agreement is slightly worse, particularly at lower $p_T(\ell\ell)$ due to the quark masses which are treated differently in CASCADE3 and PYTHIA8.

Finally, we compared the TMDs obtained by the PDF2ISR approach with the experimental data from CMS. For this comparison we turned on FSR and used the intrincis-k_T width parameter $q_s = 1.04$ GeV, which was determined in Ref. [12] to be the best fit for describing CMS data at $\sqrt{s} = 13$ TeV. The TMDs for the lower $p_T(\ell\ell)$ region, where the shape of the distribution is governed by initial state radiation effects, are shown in Fig. 9.

5 Conclusions and Outlook

In this work, we have presented a detailed study of the PDF2ISR approach, using DY pair production as a benchmark process, due to its high sensitivity to initial state parton showers. By comparing predictions obtained with PDF2ISR to those from the PB method and experimental data, we have established the validity of the approach in a realistic collider setting.

A very good agreement was observed between the DY pair $p_T(\ell\ell)$ distributions generated with the PB method and those obtained from the PDF2ISR approach. The distributions for different quark flavours confirm the consistency between the two approaches. When compared to LHC measurements, the PDF2ISR predictions provide an accurate description of the data.

Looking ahead, further validation of the PDF2ISR approach at lower centre-of-mass energies will provide important tests of its universality. In addition, the application of the method to other processes beyond DY pair production will be essential to fully exploit the potential of this approach.

Acknowledgments This article is part of a national scientific project funded by the Montenegrin Ministry of Education, Science and Innovations. We gratefully acknowledge this support.

References

[1] T. Sjöstrand et al., An introduction to PYTHIA 8.2. Comput. Phys. Commun. **191**, 159-177 (2015). https://doi.org/10.1016/j.cpc.2015.01.024

[2] C. Bierlich et al., A comprehensive guide to the physics and usage of PYTHIA 8.3. SciPost Phys. Codeb. **2022**, 8 (2022). https://doi.org/10.21468/SciPostPhysCodeb.8

[3] J. Bellm et al., Herwig 7.0 / Herwig++ 3.0 Release Note. Eur. Phys. J. C **76**, 196 (2016). https://doi.org/10.1140/epjc/s10052-016-4018-8

[4] M. Bahr et al., Herwig++ physics and manual. Eur. Phys. J. C **58**, 639-707 (2008). https://doi.org/10.1140/epjc/s10052-008-0798-9

[5] F. Hautmann et al., Collinear and TMD quark and gluon densities from parton branching solution of QCD evolution equations. JHEP **2018**, 070 (2018). https://doi.org/10.1007/JHEP01(2018)070

[6] F. Hautmann et al., Soft-gluon resolution scale in QCD evolution equations. Phys. Lett. B **772**, 446-451 (2017). https://doi.org/10.1016/j.physletb.2017.07.005

[7] G. Altarelli and G. Parisi, Asymptotic freedom in parton language. Nucl. Phys. B **126**, 298-318 (1977). https://doi.org/10.1016/0550-3213(77)90384-4

[8] H. Jung et al., A parton shower consistent with parton densities at LO and NLO: PDF2ISR. Eur. Phys. J. C **85**, 870 (2025). https://doi.org/10.1140/epjc/s10052-025-14595-y

[9] CMS Collaboration, Measurement od the mass dependence of the transverse momentum of lepton pairs in Drell-Yan production in proton proton collisions at $\sqrt{s} = 13$ TeV. Eur. Phys. J. C **83**, 628 (2023). https://doi.org/10.1140/epjc/s10052-023-11631-7

[10] CMS Collaboration, Energy-scaling behavior of intrinsic transverse momentum parameters in Drell-Yan simulation. Phys. Rev. D **111**, 072003 (2025). https://doi.org/10.1103/PhysRevD.111.072003

[11] S. Baranov et al., CASCADE3 A Monte Carlo event generator based on TMDs. Eur. Phys. J. C **81**, 425 (2021). https://doi.org/10.1140/epjc/s10052-021-09203-8

[12] I. Bubanja et al., The small k_T region in Drell-Yan production at next-to-leading order with the parton branching method. Eur. Phys. J. C **84**, 154 (2024). https://doi.org/10.1140/epjc/s10052-024-12507-0

[13] I. Bubanja et al., Center-of-mass energy dependence of intrinsic-k_T distributions obtained from Drell-Yan production. Eur. Phys. J. C **85**, 278 (2025). https://doi.org/10.1140/epjc/s10052-025-14021-3

[14] N. Raičević, Non-perturbative contributions to low transverse momentum Drell-Yan pair production using the Parton Branching Method. Phys. Scr. **100**, 045306 (2025). https://doi.org/10.1088/1402-4896/adc163

[15] I. Bubanja et al., Interplay of intrinsic motion of partons and soft gluon emissions in Drell-Yan production studied with PYTHIA. Eur. Phys. J. C **85**, 363 (2025). https://doi.org/10.1140/epjc/s10052-025-14066-4